Corticosteroid receptors adopt distinct cyclical transcriptional signatures

Florian Le Billan, Larbi Amazit, Kevin Bleakley, Qiong-Yao Xue, Eric Pussard, Christophe Lhadj, Peter Kolkhof, Say Viengchareun, Jérôme Fagart, Marc Lombes

Corticosteroid receptors adopt distinct cyclical transcriptional signatures

Florian Le Billan,[*,†] Larbi Amazit,[*,†,‡] Kevin Bleakley,[§,¶] Qiong-Yao Xue,[*,‖] Eric Pussard,[*,‖] Christophe Lhadj,[*,†] Peter Kolkhof,[#] Say Viengchareun,[*,†] Jérôme Fagart,[*,†,1,2] and Marc Lombès[*,†,,1,3]**

[*]INSERM, U1185, Le Kremlin-Bicêtre, France; [†]Univ Paris-Sud, Université Paris-Saclay, Faculté de Médecine Paris-Sud, Unité Mixte de Recherche S1185, Le Kremlin-Bicêtre, France; [‡]Unité Mixte de Service 32, Institut Biomédical de Bicêtre, Le Kremlin-Bicêtre, France; [§]Institut National de Recherche en Informatique et Automatique-Saclay, Palaiseau, France; [¶]Département de Mathématiques d'Orsay, Orsay, France; [‖]Assistance Publique–Hôpitaux de Paris (AP–HP), Hôpital de Bicêtre, Service de Génétique Moléculaire, Pharmacogénomique et Hormonologie, Le Kremlin Bicêtre, France; [#]Department of Cardiology Research, Bayer AG, Global Drug Discovery, Wuppertal, Germany; and [**](AP–HP), Hôpital de Bicêtre, Service d'Endocrinologie et des Maladies de la Reproduction, Le Kremlin Bicêtre, France

ABSTRACT: Mineralocorticoid receptors (MRs) and glucocorticoid receptors (GRs) are two closely related hormone-activated transcription factors that regulate major pathophysiologic functions. High homology between these receptors accounts for the crossbinding of their corresponding ligands, MR being activated by both aldosterone and cortisol and GR essentially activated by cortisol. Their coexpression and ability to bind similar DNA motifs highlight the need to investigate their respective contributions to overall corticosteroid signaling. Here, we decipher the transcriptional regulatory mechanisms that underlie selective effects of MRs and GRs on shared genomic targets in a human renal cellular model. Kinetic, serial, and sequential chromatin immunoprecipitation approaches were performed on the period circadian protein 1 (*PER1*) target gene, providing evidence that both receptors dynamically and cyclically interact at the same target promoter in a specific and distinct transcriptional signature. During this process, both receptors regulate *PER1* gene by binding as homo- or heterodimers to the same promoter region. Our results suggest a novel level of MR–GR target gene regulation, which should be considered for a better and integrated understanding of corticosteroid-related pathophysiology.

KEY WORDS: chromatin immunoprecipitation · kinetics · nuclear receptors · aldosterone signaling · cortisol

Aldosterone, the main mineralocorticoid hormone in humans, is involved in pleiotropic actions, of which the best characterized is the regulation of transepithelial sodium reabsorption in epithelial tissues (1). This steroid hormone is also involved in several pathophysiologic conditions as many clinical studies have linked hyperaldosteronism to major dysfunctions, notably in the cardiorenal system (2). Aldosterone acts by binding to the mineralocorticoid receptor (MR; encoded by *NR3C2* gene), a ligand-dependent transcription factor, that belongs to the nuclear receptor superfamily (3). This nuclear receptor is composed of 3 main domains, an N-terminal domain that is involved in transcriptional coregulator binding and that harbors 2 ligand-independent activating functions (AF1a and AF1b), a central DNA-binding domain (DBD), and a C-terminal ligand-binding domain (LBD) that harbors the ligand-dependent AF2 (4). In the absence of a ligand, MR forms a hetero-oligomeric chaperone complex that includes the heat shock protein, HSP90. Aldosterone binding to the cytoplasmic MR triggers its dissociation from this complex, its translocation into the nucleus, binding as a dimer to hormone response elements, and recruitment of transcriptional coregulators, which leads to the activation of MR target gene expression (4).

ABBREVIATIONS: 11βHSD2, 11β-hydroxysteroid dehydrogenase type 2; AF, activating function; ChIP, chromatin immunoprecipitation; DBD, DNA-binding domain; DCC, dextran-coated charcoal; ERα, estrogen receptor isoform α; FBS, fetal bovine serum; GR, glucocorticoid receptor; GRE, glucocorticoid responsive element; hMR, human mineralcorticoid receptor; HTM, high-throughput microscopy; LBD, ligand-binding domain; MR, mineralocorticoid receptor; PER1, period circadian protein 1; PIC, protease inhibitor cocktail; qPCR, quantitative PCR; RNA Pol II, RNA polymerase II; SRC-1, steroid receptor coactivator-1; TSS, transcription start site

[1] These authors contributed equally to this work.

[2] Correspondence: INERM U1185, Faculté de Médecine Paris-Sud, Université Paris-Sud, 63 Rue Gabriel Péri, 94276 Le Kremlin-Bicêtre, France. E-mail: jerome.fagart@inserm.fr

[3] Correspondence: INSERM U1185, Faculté de Médecine Paris-Sud, Université Paris-Sud, 63 Rue Gabriel Péri, 94276 Le Kremlin-Bicêtre, France. E-mail: marc.lombes@u-psud.fr

However, several lines of evidence suggest that mineralocorticoid signaling is much more complex than this simplistic scheme. Indeed, glucocorticoids (cortisol in humans and corticosterone in mice and rats) act as MR agonists and possess the same affinity as aldosterone for MR (5). Despite these similar affinities, MR is more sensitive to aldosterone than to glucocorticoids (6, 7). This is mainly because of an imperfect accommodation of glucocorticoids within the ligand-binding pocket of MR, which forms unstable complexes that are less productive (8); however, given that plasma levels of cortisol are 100- to 1000-fold higher than those of aldosterone, it has been suggested that MR may be fully and permanently bound by glucocorticoids (9). Epithelial tissues, classic MR targets, express the 11β-hydroxysteroid dehydrogenase type 2 enzyme (11βHSD2), which converts glucocorticoids into their 11-dehydroderivatives; cortisol into cortisone, and corticosterone into 11-dehydrocorticosterone, that are almost unable to activate MRs, which allows selective access and specific activation of MRs by aldosterone (10, 11). Moreover, it has been reported that, despite 11βHSD2 action, cortisol is not fully metabolized and is still present at a concentration at least 10 times higher than that of aldosterone (12, 13), which suggests that MR signaling in epithelial cells might be activated by both hormones. Finally, 11βHSD2 is not expressed in nonepithelial MR target tissues, such as the heart, brain, and adipose tissues, thus removing the selective protection of MRs from glucocorticoids (9).

In addition to this potential duality in ligands that are able to activate MRs, the glucocorticoid receptor (GR; encoded by *NR3C1* gene) is ubiquitously expressed (14). MR and GR display 94% sequence identity at the DBD, which allows both receptors to bind the same DNA sequence, the glucocorticoid response element (GRE) (15); however, although MRs and GRs share almost the same ligands and bind the same DNA sequences and molecular partners, including coregulators (16), they, for the most part, do not exert overlapping effects. Supporting this observation, specific gene inactivation in the mouse model led to distinct phenotypes, which is consistent with the lack of redundant and reciprocal actions. Indeed, MR and GR knockout mice died within the first days of life from massive sodium and fluid loss and from severely atelectatic and nonfunctional lung formation, respectively (17, 18).

As a result of the coexpression of both MRs and GRs, we wondered what the molecular determinants are that allow differential and selective hormone-activated signaling pathways that lead to distinct physiologic responses.

To decipher the respective contribution of both receptors and both hormones in renal corticosteroid signaling involved in the regulation of sodium reabsorption, we used HK-GFP-human MR (hMR) cells, a human renal cell line that is devoid of 11βHSD2 but that expresses both endogenous MRs and GRs, together with a fusion protein between GFP and hMR. We investigated the effect of the interaction of both receptors on the promoter of period circadian protein 1 (*PER1*), a common target gene (19–21) and demonstrated that MRs and GRs are differentially recruited in a dynamic and cyclical manner. We correlated receptor occupancy and their comprehensive kinetics, together with their interaction with steroid receptor coactivator-1 (SRC-1) and RNA polymerase type II (RNA Pol II) with the corresponding gene transactivation as a function of the nature of the ligand. Our study identifies distinct MR and GR recruitment with dissimilar genomic binding kinetics, and, using serial or tandem chromatin immunoprecipitation (ChIP) experiments, provides evidence for homodimer and MR–GR heterodimer formation that may account for specific receptor-mediated gene activation.

MATERIALS AND METHODS

Compounds and reagents

Aldosterone, cortisol, RU486, protease inhibitor cocktail (PIC), α-amanitin, and Laemmli buffer were purchased from MilliporeSigma (St. Quentin Fallavier, France). [^{3}H]Cortisol was purchased from PerkinElmer (Villebon sur Yvette, France). DMEM high glucose with L-glutamine medium, trypsin, geneticin (G418), Fast SYBR Green Master Mix, random primers, dNTP, and superscript reverse polymerase were purchased from Thermo Fisher Scientific (Villebon-sur-Yvette, France). PBS and penicillin-streptomycin solutions were purchased from GE Healthcare (Vélizy-Villacoublay, France). Western blot equipment was from Bio-Rad (Hercules, CA, USA). FluoroBrite DMEM and Hoechst 33342 were purchased from Thermo Fisher Scientific. Finerenone was provided by Dr. Peter Kolkhof (Bayer AG, Wuppertal, Germany).

Abs

Purified rabbit polyclonal SY4649 Ab was raised against and purified with the AF1a domain (residues 1–167) at the N terminus of hMR (Double X/XP Boosting Ab production program; Eurogentec, Seraing, Belgium). The hAF1a domain was expressed in *Escherichia coli* as a fusion protein with GST. After loading onto a 5-ml GSTrap column (GE Healthcare), fusion protein was cleaved *in situ* with the PreScission protease (GE Healthcare), and hAF1a recovered in the flow through and was further purified on anion exchange chromatography. Rabbit anti–SRC-1 M-341 (sc-8995 X) and anti–RNA Pol II H-224 (sc-9001 X) Abs were from Santa Cruz Biotechnology (Heidelberg, Germany). Rabbit anti-GR PA1–516 Ab was from Thermo Fisher Scientific, anti–α-tubulin was from MilliporeSigma, and the unrelated control Ab was from the iDeal ChIP-seq Kit for Transcription Factors (Diagenode, Seraing, Belgium).

Cell culture

Human renal GFP-hMR cells (HK-GFP-MR clone 20) and parental cells (HK cells) (21–24) were routinely cultured at 37°C in a humidified incubator with 5% CO_2 and seeded on Petri dishes (BP100) with 10 ml DMEM (high glucose DMEM with L-glutamine) that contained 2.5% fetal bovine serum (FBS; Biowest, Courtaboeuf, France), 100 U/ml penicillin, and 100 μg/ml streptomycin. For HK-GFP-MR cells, medium was supplemented with geneticin G418 (200 μg/ml).

Western blot analysis

Total protein extracts were prepared from parental HK or HK-GFP-MR cells using protein extraction buffer (150 mM NaCl;

50 mM Tris-HCl, pH 7.5; 0.5 mM EDTA; 30 mM sodium pyrophosphate; 50 mM NaF) that was supplemented with 1% Triton X-100, 1% PIC, and 0.1% SDS before extraction. Samples were kept at 4°C for 30 min, then centrifuged at 16,000 *g* for 20 min at 4°C. Supernatant was recovered, and protein concentrations were quantified by using the bicinchoninic acid assay (Interchim, Montluçon, France). Fifty micrograms of proteins were prepared in 4× Laemmli buffer by incubation at 95°C for 5 min. Samples were electrophoresed in a Trans-Blot SD tank (Bio-Rad), first into a stacking gel for 20 min at 120 V, then into a 7.5% separation gel for 40 min at 200 V. Proteins were transferred on a membrane using a liquid method for 1 h and 30 min at 250 mA at 4°C. Membranes were blocked for 1 h at room temperature with 5% nonfat milk in Tris-buffered saline–Tween and incubated at 4°C overnight with 1:500 anti-GRα Ab (Thermo Fisher Scientific) and 1:10,000 anti–α-tubulin (MilliporeSigma) for loading control. Membranes were rinsed 3 times with Tris-buffered saline–Tween and incubated for 1 h at room temperature with DyLight Fluor secondary Abs, rabbit 800 and Mouse 680 (1:15,000; Thermo Fisher Scientific). After 3 washes, membranes were analyzed using the Odyssey Fc imaging system (Li-Cor Biosciences, Lincoln, NE, USA).

Ligand binding assays

Forty-eight hours before collection, parental HK and HK-GFP-MR cells were washed twice with 1× PBS and placed in DMEM that contained 2.5% dextran-coated charcoal (DCC) –stripped FBS for steroid starvation. After 2 washes with ice-cold 1× PBS, cells were collected and frozen at −150°C. Cells were ground in a mortar under liquid nitrogen and resuspended in TEG-Mo buffer [20 mM Tris-HCl, 1 mM EDTA, 20 mM sodium molybdate, and 10% glycerol (v/v), pH 7.4] that was supplemented by 1% PIC. Cells were disrupted by using a Teflon-glass potter. Cell homogenates were then centrifuged at 16,000 *g* for 30 min at 4°C, and supernatants were considered as cytosolic fractions. Reticulocyte lysates were prepared as previously described (25) and diluted twice with TEG-Mo buffer. Samples were incubated for 4 h at 4°C with 20 nM [^{3}H]cortisol alone or in the presence of 500-fold excess of unlabeled cortisol, finerenone, or RU486. Bound and free ligands were separated by using the DCC method (26). Bound [^{3}H]cortisol was measured by counting the radioactivity of the supernatant and expressed in femtomoles per milligrams protein. Results are presented as means ± SEM of triplicate from 1 experiment.

Measurement of 11βHSD2 activity by liquid chromatography–tandem mass spectrometry

After 48 h of steroid starvation, HK-GFP-MR cells were incubated in DMEM that was supplemented with 2.5% DCC FBS medium that contained 100 nM cortisol or 100 nM corticosterone for 16 h. Supernatants were recovered to measure cortisol (F), cortisone (E), corticosterone (B), and 11-dehydrocorticosterone (A) concentrations by using the liquid chromatography–tandem mass spectrometry method (27). Conversion was calculated as the ratio between E/F + E (or A/B + A) before and after incubation. Results are expressed as percent conversion and are means ± SEM of 3 independent measurements.

Import kinetics and automated high-throughput microscopy

HK-GFP-MR cells were seeded in 4-well chamber slides (Sarstedt, Nümbrecht, Germany). Geneticin was removed from cell medium 5 d before experiments. Hormone withdrawal was obtained by incubating cells in serum-starved medium for 48 h and performing extensive washings with 1× PBS. Cells were then treated during 1, 3, 5, 7, 9, 11, 13, 15, 20, 30, or 45 min with 100 nM aldosterone or cortisol, then fixed with 4% paraformaldehyde (Electron Microscopy Sciences, Nanterre, France). Immunocytochemistry was performed with an anti-GFP Ab (MilliporeSigma) as previously described (24). Cytoplasmic and nuclear fluorescence intensities were quantified by high-throughput microscopy (HTM) with an Arrayscan VTI microscope (Thermo Fisher Scientific). Molecular Translocation V4 Bioapplication (vHCS Scan, v.6.3.1) was used to calculate the ratio of nuclear to cytoplasmic fluorescence, as described in our previous study (24). The live cell chamber module (Thermo Fisher Scientific) of the Arrayscan VTI was used to perform multifield videomicroscopy of GFP-hMR import kinetics for 45 min (37°C and 5% CO_2). Subcellular GFP fluorescence was observed in the presence of 100 nM aldosterone or cortisol for 45 min. Sequential acquisition of 8 fields (GFP-channel) for both conditions was performed by using an exposure time of 50 ms and a binning of 4 × 4 to minimize phototoxic effects.

Reverse transcription and Real-time quantitative PCR

HK-GFP-MR cells were washed twice with ice-cold PBS. Total RNA extraction, reverse transcription, and quantitative PCR (qPCR) were performed as previously described (21). Primers were used at a final concentration of 300 nM (see Supplemental Table 1 for primers sequence). Relative expression in a given sample was normalized to internal reference *GAPDH* mRNA values, where control condition values were arbitrarily set at 1. Results are expressed as means ± SEM of at least 3 independent experiments performed in triplicate.

ChIP

Geneticin was omitted from cell medium 5 d before experiments. Forty-eight hours before experiments, HK-GFP-MR cells were washed twice with 1× PBS and incubated in DMEM that contained 2.5% DCC FBS (step A). Cells were then incubated for 1 h at 37°C with either 1:1000 ethanol, 100 nM aldosterone, 100 nM cortisol, or 10 μM finerenone, or a combination of ligands as indicated on the corresponding figure legends, all in DMEM that was supplemented by 2.5% DCC FBS (step B). The next steps were carried out by using the iDeal ChIP-seq Kit for transcription factors according to the manufacturer's recommendations with the following modifications. During cell treatment, protein A–coated magnetic beads (30 μl of the stock suspension) were washed twice in prepared C1 buffer (4.2 ml molecular grade water, 0.8 ml iC1b, and 80 μl 5% bovine serum albumin) and finally resuspended in 30 μl of prepared C1 buffer. Precoating mix was prepared with these beads, 5 μg of one of the Abs, plus 1× PIC 100 times, and 5% bovine serum albumin (final volume 100 μl), then incubated for 4 h on a rotating wheel (40 rpm) at 4°C (step C). Cells were fixed for 10 min at room temperature by adding one-tenth fixation solution (10% paraformaldehyde in fixation buffer) to the medium. After 5 min of neutralization of the medium with the addition of 0.125 M glycine, cells were washed once with a large volume of ice-cold 1× PBS. After cell lysis, extracted chromatin was sheared in 300 μl of shearing buffer iS1b + 1× PIC 100 times and transferred into 1.5 ml Bioruptor Pico Microtubes with Caps by applying 1 run of 8 cycles (Bioruptor Pico; Diagenode). Each cycle was composed of 30 s with the effective application of ultrasound (ON) and 30 s without (OFF; step D). Sheared chromatin (250 μl) was added to precoated beads. Samples were incubated overnight at 4°C on a rotary incubator (step E). From each sample of sheared chromatin, 2.5 μl were kept aside as input material to calculate the

percentage of immunoprecipitated DNA. The next day, magnetic beads were washed and immunoprecipitated DNA was eluted. Eluted DNA and DNA from the input were next purified and recovered in 50 μl of buffer C (step F). One-quarter dilution of purified DNA was used for quantification by genomic qPCR (step G).

Kinetics experiments for ChIP analysis

During kinetics experiments for ChIP, only step B from the above protocol was modified. HK-GFP-MR cell treatment was started every 5 min according to the following steps. Cells were pre-incubated for 2 h with DMEM that was supplemented with 2.5% DCC FBS that contained 2.5 μM α-amanitin, washed twice with 1× PBS, and then treated for 0–120 min with 2.5% FBS DCC medium that contained 100 nM aldosterone or 100 nM cortisol. Each time point, condition was stopped by adding one-tenth fixation solution (10% paraformaldehyde in fixation buffer) to the medium for 10 min at room temperature.

Serial ChIP

After step E of the ChIP protocol, samples were placed on the magnetic rack for 1 min and supernatants were recovered in new tubes. These supernatants corresponded to unbound chromatin from the ChIP experiment. Step C was repeated with new magnetic beads and the appropriate Ab. Unbound chromatin was then incubated with precoated beads overnight at 4°C on a rotary incubator. Unbound chromatin (3.5 μl) was kept aside to evaluate the input. Lastly, steps F and G were performed as previously described.

Tandem ChIP

After step E from the ChIP protocol above, samples were washed 4 times as recommended in the kit protocol. Magnetic beads were resuspended in 50 μl SDS DTT Elution buffer (50 mM Tris-HCl, 10 mM EDTA, 1% SDS, 10 mM DTT, pH 7.0) and incubated for 30 min at 37°C. Eluted immunoprecipitated chromatin was recovered in a new tube and diluted to one tenth in dilution buffer (50 mM Tris-HCl, 150 mM NaCl, 5 mM EDTA, 0.1% Na-deoxycholate, 5 mM sodium butyrate, pH 8.0) completed with 1% Triton X-100, 1 mM serine protease inhibitor AESBF, and 1% PIC before dilution. Step C was repeated with new magnetic beads and the appropriate Ab. Eluted chromatin (490 μl) was then incubated with precoated beads overnight at 4°C on a rotary incubator. Unbound chromatin (4.9 μl) were kept aside to evaluate the input. Lastly, steps F and G were performed as previously described.

Genomic qPCR

Purified DNA from ChIP, kinetic ChIP, serial ChIP, and tandem ChIP were analyzed by genomic qPCR, performed in triplicate, as previously described (21). Primers were used at a final concentration of 300 nM (see Supplemental Table 1 for primers sequences). Results are expressed as means ± SEM of 3 independent experiments performed in triplicate for ChIP, and at least 1 experiment performed in triplicate for kinetic ChIP, serial ChIP, and tandem ChIP.

Statistical analysis and modeling

Experimental data are presented as means ± SEM. Statistical analyses were performed with Prism 5 software (GraphPad Software, La Jolla, CA, USA), with nonparametric Mann-Whitney *U*-tests. Values of $P < 0.05$ were considered significant, as shown in the figures. For kinetic experiments for ChIP analysis, each set of time series data was fitted using cubic smoothing splines with 23 df *via* the smooth-spline function in R software (v.3.3.2; *https://www.r-project.org/*).

RESULTS

Validation of cellular and molecular tools

To accurately investigate renal mineralocorticoid and glucocorticoid signaling, it was necessary to appropriately control experimental conditions. For this purpose, we selected the only available human renal cell line that expressed MR, HK-GFP-hMR cells, a relevant *in vitro* cellular model derived from the distal convoluted tubule [parental HK cells (22)] that has been stably transfected with an expression vector that encodes for the GFP-hMR fusion protein (23). This cell line previously allowed us to describe the hMR cistrome and to additionally characterize the mineralocorticoid signaling pathway in human renal cells (21, 24). To evaluate the relative expression level of each receptor, MR and GR, in both HK (parental) and HK-GFP-hMR cells, binding assays were performed using [^{3}H]cortisol as a common ligand for both corticosteroid receptors, together with selective antagonists, finerenone, a highly selective MR antagonist (24, 28), or RU486, a potent GR antagonist (29). *In vitro* translated hMRs or hGRs were incubated with [^{3}H]cortisol in the absence (total binding) or presence of 500-fold excess of unlabeled cortisol to quantify nonspecific binding. In parallel, reticulocyte lysates were incubated with [^{3}H]cortisol, together with 500-fold excess of finerenone that, as expected, displaced [^{3}H]cortisol binding from MRs, but not from GRs (Supplemental Fig. 1). Lysates were also incubated with [^{3}H]cortisol plus 500-fold excess of RU486, which was unable to bind MRs (30). As expected, RU486 displaced [^{3}H]cortisol binding from GRs, but not from MRs (Supplemental Fig. 1). These pivotal experiments allowed us to discriminate the binding of cortisol to MRs or GRs. Clarified cytosolic fractions from parental HK and HK-GFP-hMR cells were thereafter incubated with 20 nM [^{3}H]cortisol in the absence (total binding) or presence of 500-fold excess of unlabeled cortisol (nonspecific binding), finerenone (nonspecific plus GR binding), or RU486 (nonspecific plus MR binding). Both selective antagonists could reduce cortisol binding, which indicates that MRs and GRs were both expressed at relatively low levels in parental HK cells (estimated at ~8 fmol/mg protein; **Fig. 1*A***, left), whereas, as anticipated, MR levels were 10 times higher in HK-GFP-hMR cells (Fig. 1*A*, right) measured at 80 fmol/mg protein, with the GR expression level remaining unchanged. Expressions of endogenous MR and GFP-hMR fusion protein in HK-GFP-hMR cells were previously confirmed by Western blot analysis using our in-home anti-MR Ab (21). Western blot analysis further validated endogenous GR expression in HK-GFP-hMR and parental HK cells (94 kDa; Fig. 1*B*), as revealed by anti-GR Ab. Before performing ChIP targeting MR, we examined the ability of the SY4649 anti-MR Ab, generated

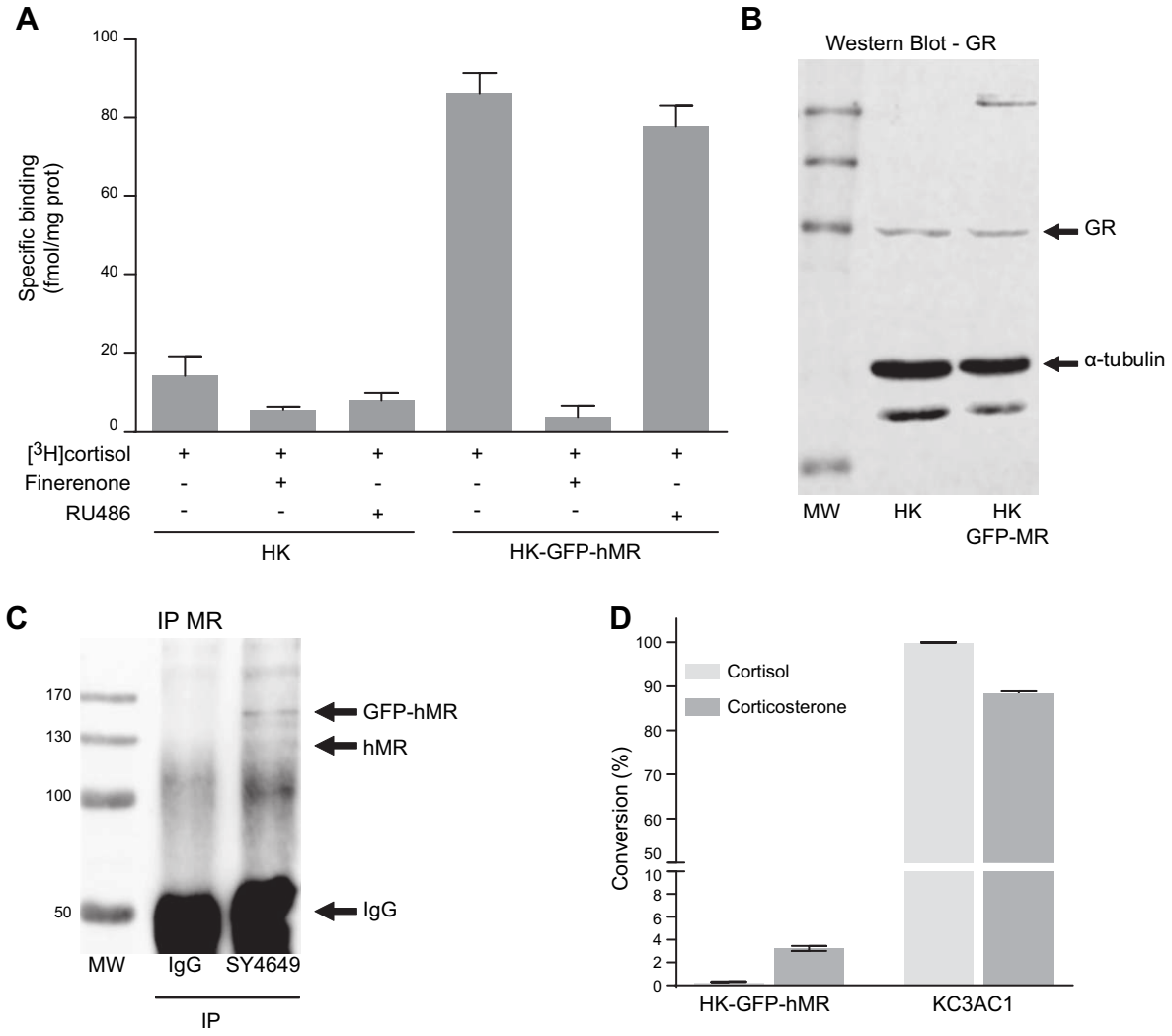

Figure 1. Characterization of HK-GFP-hMR cells. *A*) Binding assays on extracts of parental HK and HK-GFP-hMR cells. Cells were incubated with 20 nM [^{3}H]cortisol alone or in combination of 500-fold excess of cortisol, finerenone, or RU486 for 4 h at 4°C. Bound and unbound ligands were separated using the DCC method. Bound steroid was measured by counting the radioactivity in the supernatant, expressed in femtomoles per milligram protein. Specific binding, which corresponded to the fraction of bound cortisol in the extract, was calculated by subtracting from total binding values those obtained in the [^{3}H]cortisol + 500-fold excess of cortisol conditions. Results are presented as means ± SEM of triplicates from 1 experiment. *B*) Western blot analysis of GR expression in HK and HK-GFP-hMR cells. GR protein (94 kDa) was detected with the PA1-516 Ab (dilution 1:500; Thermo Fisher Scientific). *C*) Immunoprecipitation of GFP-hMR fusion protein and endogenous MR, from homogenates of HK-GFP-hMR cells, by the SY4649 anti-MR Ab or by negative control Rabbit IgG, and revelation by Western blot analysis using the SY4649 Ab (dilution 1:2000). *D*) Enzymatic conversion of cortisol and corticosterone in positive control renal KC3AC1 cells (31) and HK-GFP-hMR cells. Cells were incubated at 37°C with 100 nM cortisol or corticosterone for 16 h in a steroid-free medium. Concentrations of cortisol and its metabolite cortisone and corticosterone and its metabolite 11-dehydrocorticosterone were measured in cell supernatants using liquid chromatography–tandem mass spectrometry (27). Conversion was calculated as the ratio (%), and results are expressed as means ± SEM of 3 independent measurements.

against the AF-1 domain (1–167 N-terminal amino acids) of hMR, to immunoprecipitate hMR and GFP-hMR proteins from cytosolic extracts of HK-GFP-hMR cells. MR immunoprecipitation followed by Western blot analysis indicates that the SY4649 Ab is able to specifically immunoprecipitate hMR (~120 kDa) and GFP-hMR (~150 kDa) compared with the control IgG (Fig. 1*C*). Lastly, we investigated whether the activity of the 11βHSD2 enzyme was detected in HK-GFP-hMR cells by monitoring the conversion of cortisol or corticosterone into their keto derivatives, as quantified by liquid chromatography–tandem mass spectrometry (27). The murine renal KC3AC1 cell line, known to express the 11βHSD2 enzyme (31, 32), was used as a positive control. As illustrated in Fig. 1*D*, whereas KC3AC1 cells almost completely metabolized corticosteroid hormones during overnight incubation, <3% of the hormone could be converted in HK-GFP-hMR cells, which supports the absence of the 11βHSD2 enzyme in these cells. These results are concordant with the absence of *HSD11B2* transcripts in HK-GFP-hMR cells (Supplemental Fig. 2). Taken together, these results demonstrate that HK-GFP-MR cells express both endogenous MR and GR, the GFP-hMR fusion protein, and lack the 11βHSD2 enzyme,

which indicates that the HK-GFP-MR cell line is a suitable cell-based system with which to investigate the relative contribution of MRs and GRs in renal corticosteroid signaling. Moreover, the newly generated SY4649 anti-hMR Ab could efficiently immunoprecipitate hMR, thereby allowing additional investigation of MR recruitment to genomic targets.

Ligand-induced nuclear import kinetics of MRs are not delayed in the presence of cortisol

Nuclear translocation is a critical step that converts MRs into its transcriptionally active state. As assessed by automated HTM in our previous study (24), the majority of MR is located in the cytoplasm of HK-GFP-hMR cells when cultured in steroid-free medium for 48 h, which allows for an efficient hormone withdrawal. Indeed, only a small MR proportion is already in the nucleus before the addition of the ligand. We have also previously demonstrated that aldosterone treatment induces the rapid and complete accumulation of MR in the nuclear compartment within 1 h and that finerenone does not prevent MRs from entering into the nuclear compartment but, rather, delays its nuclear translocation (24). We thus verified whether cortisol distinctively modulates the subcellular trafficking of MRs. To exclude the possibility that MRs could be imported in the nuclear compartment faster in the presence of aldosterone than in the presence of cortisol, we designed a kinetic experiment to observe the subcellular localization of MRs in both conditions. Cells were incubated with either aldosterone or cortisol for various periods of time. After fixation, cells were analyzed for immunocytochemistry, and immunofluorescence was precisely quantified in cytoplasmic and nuclear compartments using HTM (500 cells per condition and time point). Visual comparison of the receptor localization under both conditions does not indicate clear-cut differences in the subcellular localization of MR, which seems to be almost completely translocated after 15 min (**Fig. 2*A*** and Supplemental Videos 1 and 2). HTM quantification and statistical analyses at different time points revealed no significant difference in the

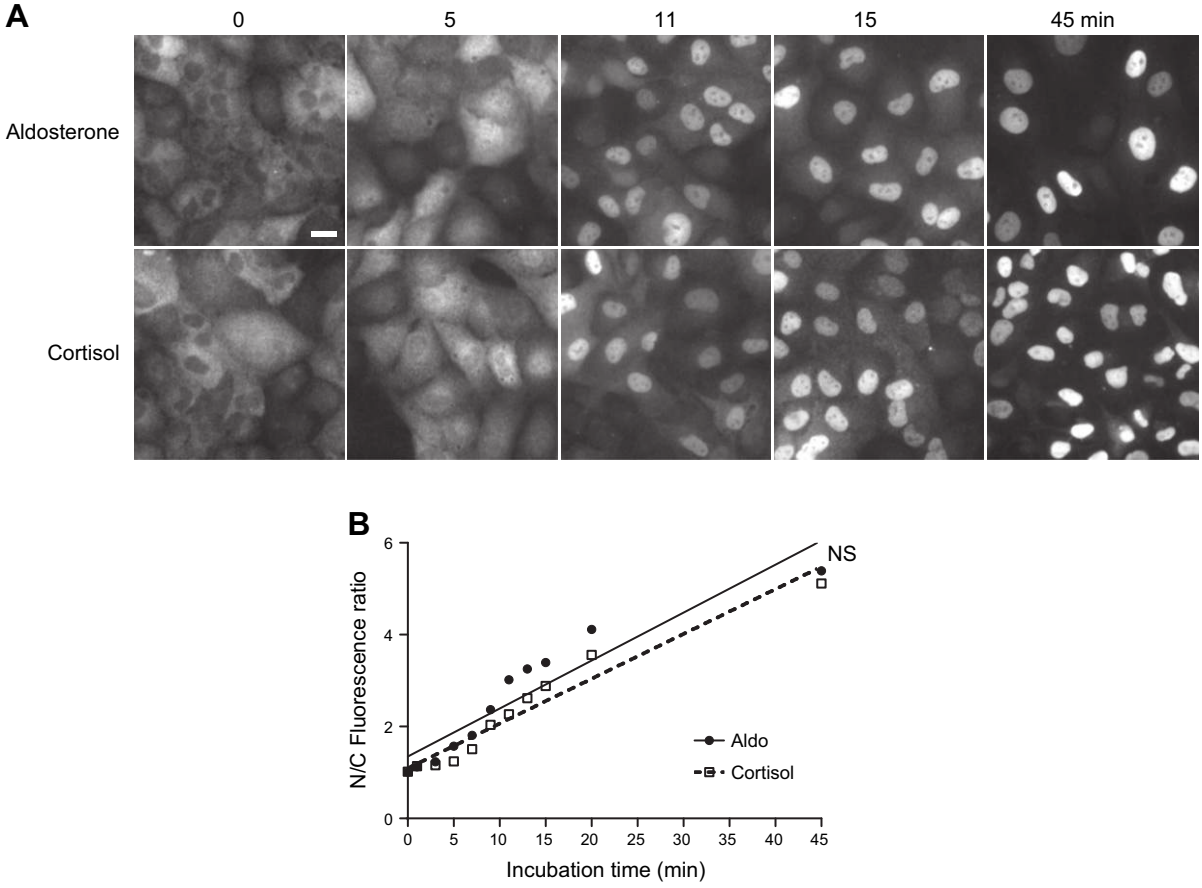

Figure 2. Aldosterone and cortisol induce nuclear translocation of GFP-hMR. HK-GFP-MR cells were incubated with 100 nM aldosterone or cortisol during the indicated time (from 0 to 45 min). Cells were fixed and MR subcellular localization was analyzed by automated microscopy on >500 cells per condition (Materials and Methods). *A*) Representative fields of GFP-hMR subcellular localization. White bar represents 20 μm for all panels. *B*) Variation of the nuclear/cytoplasmic (N/C) fluorescence ratio as a function of time (min). GFP-hMR was rapidly translocated into the nuclear compartment upon exposure to aldosterone (●, solid line) or cortisol (□, dashed line). Each point represents the mean value of the N/C ratio ± SEM. Note that SEM values are small and not visible on the graph. Linear regression by GraphPad software determined the best fit value of the slopes: aldosterone $y = 0.1044x + 1.346$ ($r^2 = 0.885$); and cortisol $y = 0.0975x + 1.088$ ($r^2 = 0.948$). Slopes were not statistically different (NS; $P = 0.645$), which indicates that the initial velocity of the nuclear import of GFP-hMR was identical in both ligands.

nuclear import rate of MRs, irrespective of the nature of the ligand (Fig. 2*B*). Altogether, these data demonstrate that, in our cellular model, the kinetics of the ligand-induced nuclear import of MRs is not delayed in the presence of cortisol, and that, consequently, both hormones, aldosterone and cortisol, are capable of inducing a similar nuclear import velocity of the receptor.

PER1 transactivation upon MR or GR agonist and antagonist exposure

We next evaluated the respective contributions of MRs and GRs in transactivating a given endogenous gene. We and others have previously identified *PER1*, a major player in the intracellular endogenous gene clock, as a renal MR target gene (19, 21, 33, 34). Moreover, some studies have reported a direct link between GRs and the circadian clock (35, 36). We therefore examined the expression level of *PER1* mRNA after treating cells for 1 h with increasing concentrations of aldosterone or cortisol in the absence or presence of 100-fold excess of finerenone or RU486. The level of *PER1* transcripts increases in a dose-dependent manner after aldosterone or cortisol stimulation (**Fig. 3*A***). Furthermore, aldosterone-induced transactivation of *PER1* was totally abolished in the presence of finerenone (Fig. 3*B*), which demonstrates that aldosterone action is specifically mediated by MRs. RU486 does not significantly impair aldosterone-induced *PER1* transactivation, which suggests that aldosterone-activated GRs are not pivotal for *PER1* transcriptional activation. Likewise, after cortisol treatment, *PER1* transcript levels significantly increased 2-fold (Fig. 3*C*). This cortisol-stimulated transactivation was inhibited by RU486, but not by finerenone; however, the combination of finerenone and RU486 significantly reduces cortisol-stimulated transactivation, which reflects a concomitant action of cortisol-activated MRs and cortisol-activated GRs under such conditions. This supports the proposal of a synergetic action of both receptors. Collectively, these results indicate that both MRs and GRs transactivate *PER1* in response to their cognate ligands, which suggests that both receptors might bind to common regulatory sequences within the same target locus in HK-GFP-hMR cells. This enables us to examine, in this cell-based system, the specific, concomitant, synergistic, or competitive recruitment of MRs and GRs onto a common and presumably unique hormone response element.

Involvement of MRs and GRs in *PER1* regulation

We next examined whether MRs and GRs are directly and physically involved in *PER1* transactivation. We have previously identified and characterized a mineralocorticoid binding sequence that contains a mineralocorticoid response element located 2044 bp upstream of the transcription start site on the promoter region of *PER1* (21). The same locus was previously identified as a glucocorticoid target (20, 37); therefore, we performed ChIP qPCR experiments on chromatin that was extracted from HK-GFP-hMR cells that were treated with agonists and/or antagonists of both receptors. Aldosterone induced strong MR recruitment onto the *PER1* promoter (an 88-fold increase; **Fig. 4*A***), which was inhibited, in part, by a 10-fold excess of finerenone. Cortisol also increased MR recruitment onto the *PER1* promoter (65-fold increase), which was significantly reduced by a factor of 3.5 in the presence of finerenone. In parallel, GR recruitment onto the same regulatory sequence located in the *PER1* promoter was enhanced after cortisol exposure (84-fold increase) and inhibited by RU486 cotreatment (3.3-fold reduction; Fig. 4*B*). Furthermore, aldosterone, which acts as a weak GR agonist (7), also promoted GR enrichment (50-fold increase). It is worth noting that RU486 alone significantly promoted GR recruitment (28-fold increase), which indicates that GR–RU486 complexes are able to bind DNA, as previously reported (38). These MR and GR recruitments are sequence specific, as no recruitment was observed on a negative control region located at +1068 bp from the *SCNN1A* transcription start site (Supplemental Fig. 3) (21). In summary, after 1 h of treatment, both aldosterone and cortisol promoted MR and GR recruitment onto the same target sequence to a comparable extent, accompanied by the subsequent transactivation of *PER1* in HK-GFP-hMR cells.

Dynamic kinetics of the recruitment of MRs, GRs, and their transcriptional partners

It has been previously shown that the transactivation efficiency of MRs and GRs in response to mineralocorticoid and glucocorticoid hormones is highly dependent on the nature of the bound hormone, with MRs being more sensitive to aldosterone than cortisol, and, conversely, GRs being more sensitive to cortisol than aldosterone (7, 39). These differences in receptor sensitivity were directly related to the stability of hormone–receptor complexes. Aldosterone–MR complexes are more stable than those that involve cortisol, and, conversely, GRs form more stable complexes with cortisol than with aldosterone (7). It has been reported that, although activated by E_2, the estrogen receptor isoform α (ERα) and its transcriptional partners are recruited to DNA in a dynamic and cyclical manner (40). Globally, assembly of the transcriptional preinitiation complex, including numerous transcription factors, follows a dynamic, cyclical, and ordered pattern, referred to as the transcriptional clock (41). Thus, to precisely discriminate the respective contribution of MRs and GRs in *PER1* activation, we examined a potential time-dependent recruitment of MRs and its molecular partners (SRC-1 and RNA Pol II). Moreover, we compared the dynamic of MR and GR recruitment onto the same GRE identified in the promoter of *PER1* as a function of the nature of the bound ligand (aldosterone *vs.* cortisol). We performed sequential ChIP experiments on HK-GFP-hMR cells that were previously synchronized by 120 min of α-amanitin exposure. This treatment was required to clear active promoters of any transcription factors (42). As demonstrated in 2 independent experiments and illustrated in **Fig. 5*A***, recruitment of aldosterone-activated MRs greatly varies over a 120-min period in a cyclic and

dynamic manner. Of particular interest, MR recruitment seems to follow 2 phases, the first is composed of 3 short cycles of approximately 10–15 min, and the second of 2 longer cycles of approximately 20–25 min. Note that no MR recruitment was observed on a genomic negative control region (Supplemental Fig. 4*A*). This finding is not specific to *PER1*, as similar MR recruitment was observed on the well-known aldosterone-regulated target gene, *SCNN1A*, with the recruitment of MR following a similar pattern, as shown in **Fig. 6*A***. Meanwhile, we addressed the question of the potential consequences of these 2 dynamic phases in MR capacity to promote transcriptional partner corecruitment. ChIP experiments performed with specific Abs demonstrated that SRC-1 enrichment onto the *PER1* promoter similarly fluctuates upon aldosterone (Fig. 5*B*). Indeed, results show several cycles that directly overlap those observed for MR (Fig. 5*A*), which suggests a corecruitment of both proteins at the promoter level. Of note, RNA Pol II binding to the *PER1* promoter also followed a cyclic rhythm, with 2 successive phases of ~60 min. Of note, RNA Pol II recruitment seems to be shifted by ~8 min compared with that of MR and SRC-1, which results in 3 short cycles of ~15 min and 2 cycles of ~20–25 min (Fig. 5*C*). These results suggest that MR and SRC-1 corecruitment is a prerequisite for RNA Pol II functional positioning into an operative preinitiation complex onto this locus.

We then assessed whether aldosterone or cortisol promotes MR and/or GR recruitment onto the *PER1* promoter with different dynamic patterns. To examine this, we performed sequential ChIP experiments on HK-GFP-hMR cells that were treated with cortisol. Unlike with aldosterone (Fig. 6*A*), cortisol seems to induce a distinct cyclic MR recruitment with shorter cycles, including an initial phase composed of 3 cycles of ~15 min, and a second that consists of 4 cycles of ~10 min (Fig. 6*B*). Although the discrepancies observed in the dynamics of recruitment (Figs. 5*A* and 6*A* *vs.* Fig. 6*B*), efficient transcription of *PER1* was obtained in the presence of aldosterone-bound MRs or cortisol-bound GRs, as shown in Fig. 3. These differences in recruitment kinetics after cortisol treatment, as opposed to aldosterone, led us to address whether the GR– and MR–cortisol complexes have similar DNA binding kinetics as a result of the fact that both MRs and GRs stimulated *PER1* mRNA expression. As illustrated in Fig. 6*C*, GR–cortisol complexes also bind the *PER1* and *SCNN1A* promoters in a cyclic-dependent manner, yet with distinct dynamic patterns as observed for MR–aldosterone (Figs. 5*A* and 6*A*). GR–cortisol complexes seemed to have a single-phase variation with a short frequency of ~10–15 min. Here, again, no GR recruitment was observed in the control genomic region (Supplemental Fig. 4*B*). Taken together, these observations indicate that both receptors

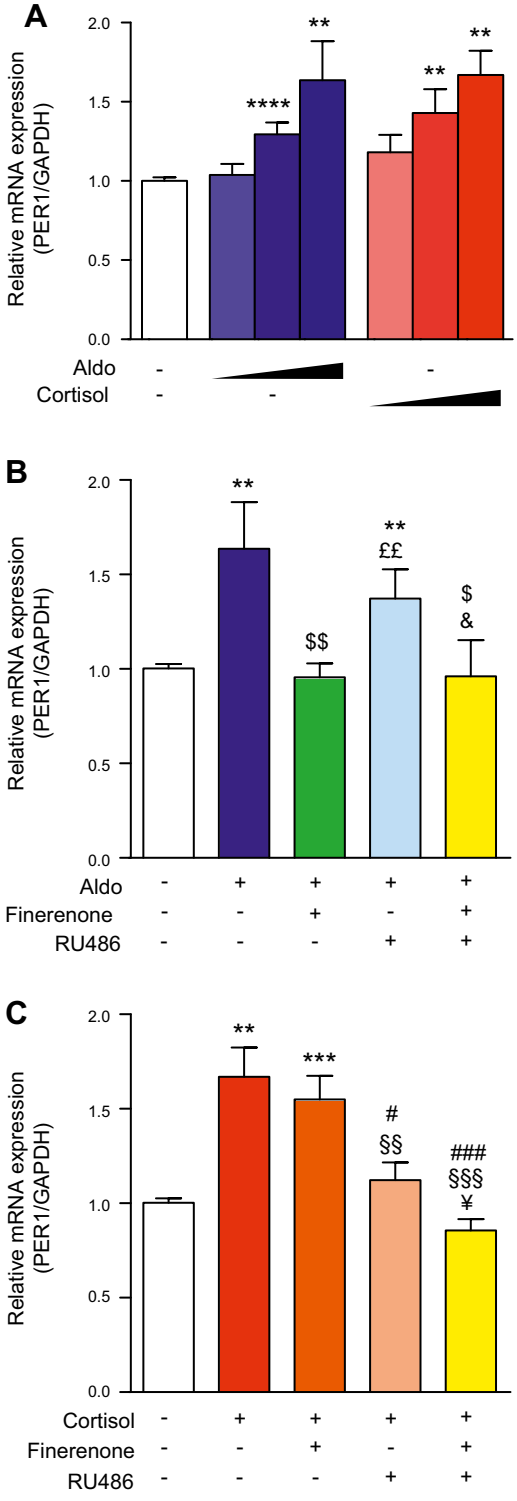

Figure 3. Transcriptional activation of *PER1* in HK-GFP-MR cells under exposure to MR and GR agonists or antagonists. After 48 h of steroid deprivation, HK-GFP-MR cells were treated for 1 h with different treatments. *A*) Cells were treated with 1, 10, or 100 nM aldosterone (Aldo) or cortisol. *B*) Cells were treated with 100 nM aldosterone, alone or in combination with 10 μM finerenone or RU486. *C*) Cells were treated with 100 nM cortisol, alone or in combination with 10 μM finerenone or RU486. Total RNAs were extracted and reverse transcribed, and relative *PER1* expression levels were quantified using qPCR using specific primers for *PER1*. Data are presented as means ± SEM of 1 experiment performed in triplicate. Statistical significance was calculated with Mann-Whitney nonparametric *U* tests. $^{**}P < 0.01$, $^{***}P < 0.001$, $^{****}P < 0.0001$ *vs.* vehicle condition, $^{\$}P < 0.05$, $^{\$\$}P < 0.01$ *vs.* aldosterone condition, $^{\pounds\pounds}P < 0.01$ *vs.* aldosterone + finerenone condition, $^{\&}P < 0.05$ *vs.* aldosterone + RU486 condition, $^{\#}P < 0.05$, $^{\#\#\#}P < 0.001$, $^{\#\#\#\#}P < 0.0001$ *vs.* cortisol condition, $^{\S\S}P < 0.01$, $^{\S\S\S}P < 0.001$ *vs.* cortisol + finerenone condition, $^{¥}P < 0.05$ *vs.* cortisol + RU486 condition.

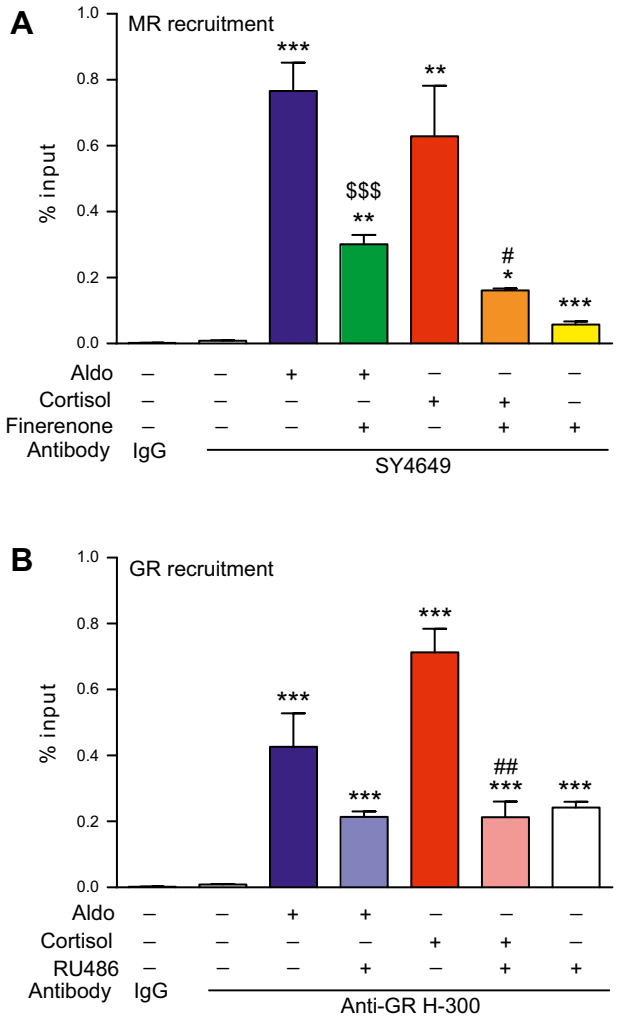

Figure 4. Ligand-induced MR and GR recruitment at the *PER1* promoter. After 48 h of steroid deprivation, HK-GFP-MR cells were treated as indicated for 1 h with 1:1000 ethanol (V), 100 nM aldosterone (Aldo), 100 nM cortisol, 1 μM finerenone, or 1 μM RU486, alone or in combination. Cells were fixed with paraformaldehyde and lysed. *A*, *B*) After shearing, chromatin extracts were immunoprecipitated with the anti-MR SY4649 Ab (*A*) or anti-GR H-300 Ab (*B*), or by the negative control rabbit IgG (*A*, *B*). Eluted and purified DNA were quantified by qPCR, with primer pairs encompassing the *PER1* promoter's GRE. Data are expressed as percent input and are means ± SEM of 3 independent experiments performed in triplicate. Ns, not significant *vs.* vehicle. Statistical significance was calculated using the Mann-Whitney nonparametric *U* tests. $^{*,\$}P < 0.05$, $^{**,\#\#}P < 0.01$, $^{***,\$\$\$}P < 0.001$ *vs.* *vehicle, $^{\$}$aldosterone, or $^{\#}$cortisol condition.

are recruited on their target promoters, with differential kinetic signatures that are highly and specifically dependent on the receptor and ligand.

Selectivity of MRs and GRs binding to GRE within the *PER1* regulatory sequence

From the above findings, we hypothesized that: *1*) upon aldosterone and cortisol stimulation, both MRs and GRs participate in the transactivation of endogenous *PER1* in HK-GFP-hMR cells, and *2*) they act, at least in part, *via* recruitment onto the same *PER1* regulatory sequences. For this reason, we next studied whether MRs and/or GRs bind separately as homodimers to activate transcription or if heterodimers between MRs and GRs also actively control gene expression. If MR and GR homodimers are formed in the presence of hormone, each one should be immunoprecipitated independently from the other. In contrast, if heterodimers do exist, immunoprecipitating one receptor should lead to the coimmunoprecipitation of the other. Therefore, a first ChIP experiment was performed on agonist-treated HK-GFP-hMR cells by taking MRs as bait, and unbound chromatin was assessed for its ability to be immunoprecipitated using the anti-GR Ab (serial ChIP experiment). Aldosterone treatment allowed for MR recruitment, and the serial ChIP experiment on unbound chromatin also revealed GR recruitment, which suggests that MRs and GRs are able to bind DNA independently from each other, presumably *via* homodimer formation (**Fig. 7*A*, *B***, see control GR recruitment in Supplemental Fig. 5*A*). Independent recruitment of MRs and GRs in the presence of the ligand was additionally confirmed by performing the same experiment in the presence of cortisol (ChIP GRs and then serial ChIP MRs on unbound chromatin, Fig. 7*D*, *E*; see control cortisol–MR recruitment in Supplemental Fig. 5*D*). We next tested the hypothesis of MR–GR heterodimerization by performing tandem ChIP experiments. After MR ChIP assays, chromatin was eluted, then assessed for its ability to be immunoprecipitated by the anti-GR Ab. MR-immunoprecipitated chromatin could be re-ChIPed by the anti-GR Ab, which indicates that MR and GR interact as heterodimers at the promoter level (Fig. 7*C*). The same experiment performed in the presence of cortisol demonstrated that, after a ChIP on GRs, chromatin was reprecipitated by using the anti-MR Ab, which confirms MR and GR heterodimer formation (Fig. 7*F*). These above observations are related to the *PER1* promoter GRE and are locus specific as no recruitment of any homodimers or heterodimers was observed on a negative control region (Supplemental Fig. 6). Taken together, these results indicate that MRs and GRs are concomitantly recruited onto the *PER1* promoter as homodimers, and that MR–GR heterodimers also interact with genomic targets.

DISCUSSION

In the current study, we provide new insights into how the corticosteroid signaling pathway is physiologically controlled by its natural hormone. A human renal cell line that expresses both functional MRs and GRs, but that lacks the 11βHSD2 enzyme, was used to examine the respective contribution of inducing a rapid and indistinguishable nuclear translocation of MRs as well as the homo- or heterodimer recruitment of these receptors to a common hormone responsive element sequence located in *PER1* and *SCNN1A* target genes. This binding is accompanied by the corecruitment of the transcriptional coregulator, SRC-1, and chronologically followed by the binding of RNA Pol II to the promoter sequence. Finally, discrepancies between aldosterone and cortisol were

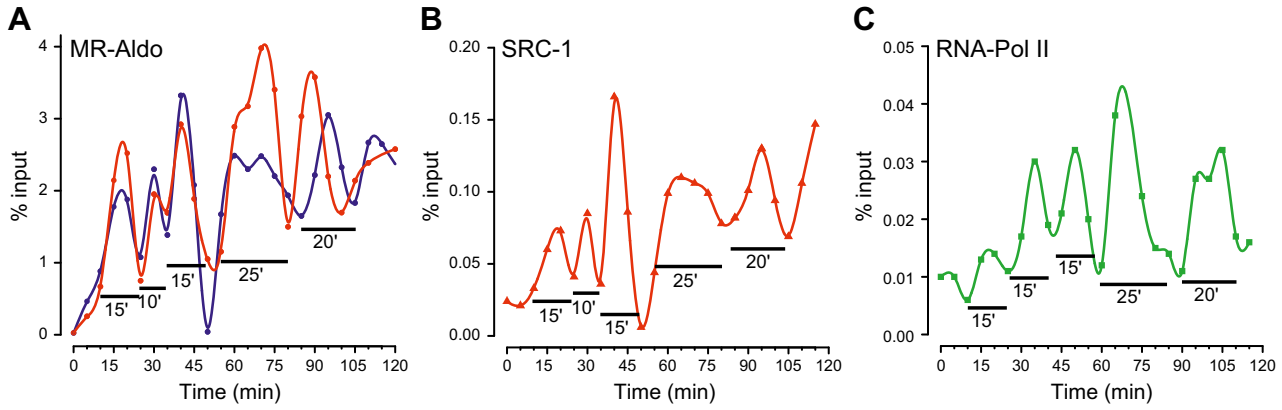

Figure 5. Cyclic and ordered recruitment of MR, SRC-1, and RNA Pol II at the *PER1* promoter. After 48 h of steroid deprivation and 2 h of pretreatment with 2.5 μM α-amanitin, cells were washed and incubated in media that was supplemented with 2.5% DCC FBS that contained 100 nM aldosterone. *A–C*) Chromatin was then prepared on sampled cells at 5-min intervals for 120 min. ChIP experiments were performed by using the anti-MR SY4649 Ab (*A*), anti-SRC-1 M-341 Ab (*B*), or the anti-Pol II H-224 Ab (*C*). The amount of immunoprecipitated *PER1* promoter was quantified by qPCR. Values, expressed as percent input, are for 2 (*A*, red and blue lines) or 1 (*B*, *C*) experiments performed in triplicate. Circles, triangles, and squares represent raw data, and lines represent fitted spline curves.

characterized and depicted in several kinetic ChIP experiments in which we demonstrate that the 2 hormones distinctively drive the cyclical and sequential transcriptional recruitment of both corticosteroid receptors. We also establish that each cyclic binding of receptors gives rise to productive transcriptional complexes as shown by the significant increase of *PER1* mRNA measured by qPCR. We also provide evidence that MRs and GRs are recruited as both homodimers and heterodimers.

Transcriptional regulation by nuclear receptors is a dynamic process that is gene and cell specific (43, 44). This phenomenon has been described according to 2 temporal scales: fast protein–DNA interaction (ms) accessible through single-living-cell fluorescent approaches (45), and global bursts of a whole receptor population binding *via* ChIP (40). In the current study, we demonstrate that MR is recruited onto the *PER1* promoter in a dynamic and cyclical manner. We also observe a concomitant recruitment of SRC-1, which is associated with an 8-min delayed recruitment of RNA Pol II. Results are consistent with those reported by Métivier *et al.* (40) for ERα, yet with some remarkable differences. The first cycle of ERα recruitment onto the promoter of *pS2* occurs after 20 min but seems to be unproductive given that neither SRC-1, nor RNA Pol II are corecruited at the promoter level. In contrast, we have demonstrated that the first cycle of MR recruitment occurs as early as after 15 min and is presumably productive because both SRC-1 and RNA Pol II are corecruited. Such a discrepancy could be explained by distinct chromatin conformations. We have previously shown that *PER1* is an early target gene, being transcribed after 30 min of hormone exposure, which suggests that chromatin on this locus might

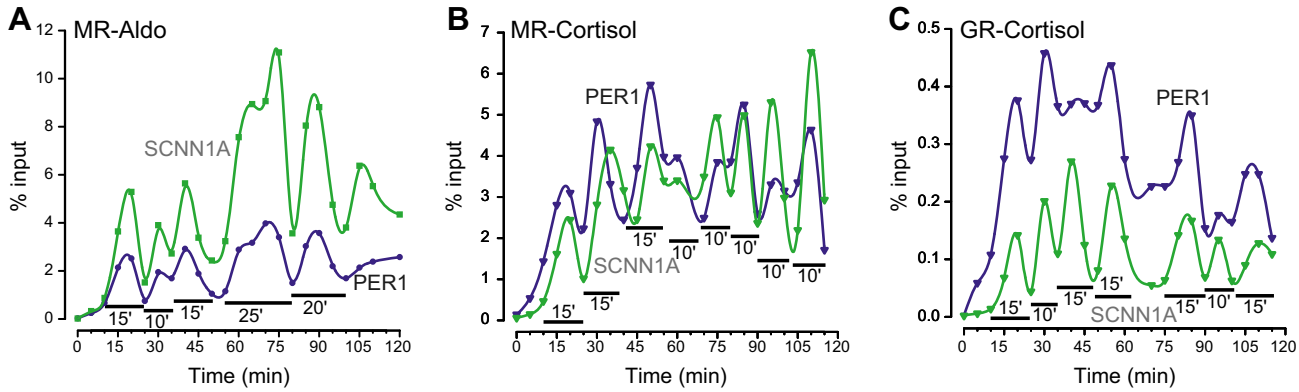

Figure 6. Dynamics of MR and GR recruitment at the *PER1* promoter. After 48 h of steroid deprivation and 2 h of treatment with 2.5 μM α-amanitin, cells were washed and incubated in media that was supplemented with 2.5% DCC FBS that contained 100 nM aldosterone or cortisol. Chromatin was then prepared on sampled cells at 5-min intervals for 120 min. ChIP experiments were performed by using the anti-MR SY4649 Ab (*A*, *B*) or the anti-GR H-300 Ab (*C*). The amount of immunoprecipitated *PER1* and *SCNN1A* promoters was quantified by qPCR. Values, expressed as percent input, are means ± SEM of 1 experiment where each sample was quantified in triplicate. Blue and green points represent raw data for *PER1* and *SCNN1A* promoters, respectively, and blue and green lines represent fitted spline curves for *PER1* and *SCNN1A*, respectively.

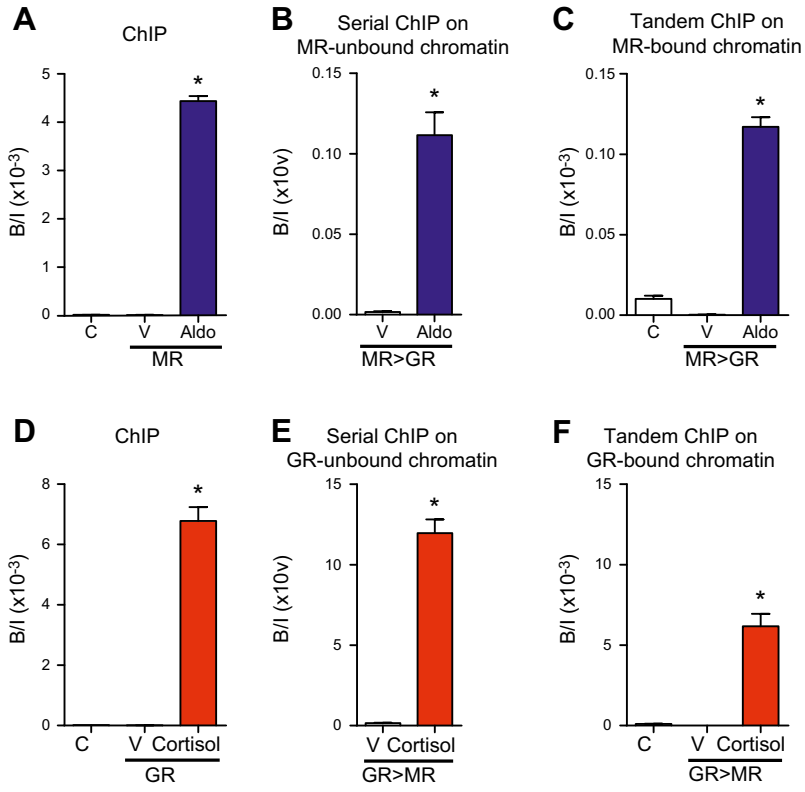

Figure 7. Homo- and heterodimerization of MR and GR at the *PER1* promoter. Forty-eight hours after steroid deprivation, HK-GFP-MR cells were treated for 1 h by 1:1000 ethanol (V), 100 nM aldosterone (Aldo), or 100 nM cortisol. Cells were fixed with paraformaldehyde and lysed. *A*, *D*) After shearing, chromatin extracts were assayed for ChIP by using the anti-MR SY4649 Ab (*A*), anti-GR H-300 Ab (*D*), or the negative control rabbit IgG (abbreviated as C in all panels). The next day, MR or GR unbound and bound chromatin were assayed by serial ChIP and tandem ChIP experiments, respectively (left panels). Serial ChIP is shown in the middle panels. *B*) MR–unbound chromatin was used for a new ChIP experiment with the anti-GR H-300 Ab. *E*) GR–unbound chromatin was used for a new ChIP experiment with the anti-MR SY4649 Ab. Tandem ChIP is shown in the right panels. *C*) MR–bound chromatin was eluted and reimmunoprecipitated by the anti-GR H-300 Ab or negative control rabbit IgG. *F*) GR–bound chromatin was eluted and reimmunoprecipitated by the anti-MR SY4649 Ab or negative control rabbit IgG. Eluted and purified DNA was quantified by qPCR using a primer pair that encompassed the *PER1* promoter's GRE (all panels). Data are expressed as enrichment (bound/input B/I) and are means ± SEM of 2 independent experiments performed in triplicate. Statistical significance was calculated with Mann-Whitney nonparametric *U* tests. $*P < 0.05$ *vs.* vehicle.

be in an euchromatin state under basal conditions (hypomethylated and hyperacetylated) (21). In contrast, *pS2* is only transcribed after 3 h of E_2 treatment in MCF-7 cells used by Métivier *et al*, which supports the notion that, under basal conditions, at least part of the gene is in a heterochromatin state. In addition, histone methyltransferases (Tip60, PRMT1), helicase Brg1, and histone acetyltransferases are rapidly recruited onto the *pS2* promoter, which is consistent with a rapid switch from a heterochromatin to a euchromatin state (40, 41). It has to be noted that, in the present study, we have only examined total RNA Pol II, whereas it has been shown that RNA Pol II activity depends on its hormone-modulated phosphorylation state (46–48). Using an anti-Ser2 phosphorylated RNA Pol II Ab during kinetic ChIP experiments would allow for the targeting of the transcriptionally active form of the enzyme (46).

Of note, the dynamic events we describe in the current study were performed in HK-GFP-hMR cells after α-amanitin synchronization, as performed previously (40). α-Amanitin is an RNA Pol II inhibitor that resets active promoters. It was observed that the first cycle is effective when cells were not treated by α-amanitin (RNA Pol II recruitment) (42); therefore, it is possible that HK-GFP-hMR cells are less sensitive to α-amanitin exposure than MCF-7 cells, which results in a faster recovery after α-amanitin washout.

It has to be pointed out that, even if MRs and ERα are cyclically recruited, oscillations do not seem to display the same frequencies. ERα recruitment followed 40- to 45-min oscillations, whereas MR recruitment after aldosterone exposure follows 2 phases of 10- to 15- and 20- to 25-min cycles. These differences could be related to different cellular, promoter, and receptor contexts. We also observed differences between the aldosterone- and cortisol-induced recruitment of MR. Aldosterone–MR recruitment on the *PER1* promoter followed 2 phases of 10- to 15- and 20- to 25-min cycles, whereas cortisol–MR recruitment had faster oscillations of 12–15 min. It has been reported that, even if aldosterone and cortisol share the same affinity for MRs, the corresponding complexes have distinct stabilities, with MR–aldosterone complexes being more stable than those that involve cortisol (7). Thus, the greater stability of the MR–aldosterone complexes could favor a longer residence time on DNA than for MR–cortisol complexes, which results in more sustained recruitment and oscillations. Also of note is that GR–cortisol complexes are even less stable than those that involve MRs (7). This could explain the rapid oscillation of cortisol-bound GR recruitment compared with that of the aldosterone– and cortisol–MR complexes. Hence, different recruitment dynamics for the 2 receptors might be considered as a new molecular mechanism, which accounts for their distinct and selective transcriptional effects.

The 2 corticosteroid receptors, MRs and GRs, as a result of their high sequence identity, notably at their DBD, share the same dimerization loop and interact with the same response element (mineralocorticoid response element/GRE). In the current study, we have shown that, after 1 h of hormone exposure (aldosterone or cortisol), the MR-bound *PER1* promoter could be reimmunoprecipitated with an anti-GR Ab and *vice versa*. Results indicate that

MRs and GRs concomitantly bound to the *PER1* promoter and suggest that both receptors interact, directly or indirectly, with this promoter which contains a unique palindromic GRE (21); however, these observations do not give any indication as to the conformation adopted by these receptors. It has long been known that MRs or GRs can act as homodimers and heterodimers through the dimerization loop (49–51). Additional experiments are needed to characterize the specific role of heterodimer MR–GR on common genomic targets.

Previous studies have suggested that MRs and GRs, acting as heterodimers, have a synergic effect on the transregulatory activity of each receptor (52, 53). Moreover, the nature of the bound ligand clearly impacts the receptor residence time on DNA, as suggested by our results and those of other studies (53, 54). These allosteric effects directly dictate the recruitment of transcriptional partners and govern the transcriptional output; therefore, homo- and heterodimerized receptors bound to a specific ligand could influence the dynamic recruitment of each other. In addition, it has been reported that aldosterone binding to MRs triggers a receptor transconformation, which allows for its N-terminal domain and LBD to interact, whereas cortisol inhibited this process (55). This N–C-terminal interaction could hypothetically involve intra- or intermolecular contacts within homodimers and heterodimers in a head-to-tail conformation, each monomer being bound to one half-site of the GRE (55).

It has also been demonstrated that GRs may form a homotetramer through both DBD and LBD interactions, only if 1 dimer is already bound to DNA (56). We now know that most transcription regulatory regions are located at large distances from transcription start sites, and that transregulation may occur through chromatin loops (57–59); therefore, we hypothesize that 1 homo- or heterodimer bound to a distal GRE enhancer could act *via* a chromatin loop, which allows for the opening of the promoter region of a target gene, whereas another dimer may bind to a more proximal GRE. Both homo- or heterodimers would then form a tetramer to stabilize the entire locus in a transcriptionally active state. Collectively, our results led us to propose new levels of interaction between MR and GR to regulate their common genomic targets, including higher oligomeric levels and more complex chromatin structures.

Overall, this study brings to light novel elements in the corticosteroid signaling pathway. The exact role of cortisol–MR complexes in the pathogenesis of diverse human diseases is not yet understood. Although the ability of tissues to regulate bioactive corticosteroid concentrations through 11βHSD isozymes is well established, it is now suggested that 11βHSD2 reduces cortisol excess only by 90% (60), which raises the question of how the remaining glucocorticoid hormone may (patho)physiologically activate the MR signaling pathway. This is even more puzzling in cells that lack 11βHSD2, such as cardiomyocytes, neurons, adipocytes, or macrophages. Herein, we describe the integrated chromatin recruitment of corticosteroid receptors in the presence of aldosterone or cortisol, with MRs and GRs able to bind with different kinetics to the genome. Thus, distinct cyclical processes may induce different transcriptional outputs as a function of the nature of the ligand with the receptor in a cell and promoter-specific manner. Our findings open new, exciting possibilities and may have pharmacologic implications in that MR or GR agonist or antagonist treatment should take into account the cyclic and dynamic transcriptional clocks for a better chronobiologic management of corticosteroid-related disorders. FJ

ACKNOWLEDGMENTS

The authors acknowledge funding from Bayer AG (P1155.0) and HAC Pharma (P1156.0). F.L.B. is the recipient of a doctoral fellowship from the Ministère de l'Enseignement Supérieur et de la Recherche. This work was supported by INSERM, Université Paris-Sud, and the Agence Nationale de la Recherche (ANR Calsignaldo; ANR-15-CE14-0005). P.K. is a full-time employee of Bayer AG. The authors declare no conflicts of interest.

AUTHOR CONTRIBUTIONS

F. Le Billan, L. Amazit, J. Fagart, and M. Lombès designed research; F. Le Billan, L. Amazit, Q.-Y. Xue, E. Pussard, C. Lhadj, J. Fagart, and M. Lombès performed research; F. Le Billan, L. Amazit, K. Bleakley, E. Pussard, J. Fagart, and M. Lombès analyzed data; F. Le Billan, L. Amazit, K. Bleakley, J. Fagart, and M. Lombès wrote the paper; and all authors analyzed the results and corrected and approved the final version of the manuscript.

REFERENCES

1. Terker, A. S., and Ellison, D. H. (2015) Renal mineralocorticoid receptor and electrolyte homeostasis. *Am. J. Physiol. Regul. Integr. Comp. Physiol.* **309**, R1068–R1070
2. Jaisser, F., and Farman, N. (2016) Emerging roles of the mineralocorticoid receptor in pathology: toward new paradigms in clinical pharmacology. *Pharmacol. Rev.* **68**, 49–75
3. Nuclear Receptors Nomenclature Committee. (1999) A unified nomenclature system for the nuclear receptor superfamily. *Cell* **97**, 161–163
4. Viengchareun, S., Le Menuet, D., Martinerie, L., Munier, M., Pascual-Le Tallec, L., and Lombès, M. (2007) The mineralocorticoid receptor: insights into its molecular and (patho)physiological biology. *Nucl. Recept. Signal.* **5**, e012
5. Arriza, J. L., Weinberger, C., Cerelli, G., Glaser, T. M., Handelin, B. L., Housman, D. E., and Evans, R. M. (1987) Cloning of human mineralocorticoid receptor complementary DNA: structural and functional kinship with the glucocorticoid receptor. *Science* **237**, 268–275
6. Lombes, M., Kenouch, S., Souque, A., Farman, N., and Rafestin-Oblin, M. E. (1994) The mineralocorticoid receptor discriminates aldosterone from glucocorticoids independently of the 11 beta-hydroxysteroid dehydrogenase. *Endocrinology* **135**, 834–840
7. Hellal-Levy, C., Couette, B., Fagart, J., Souque, A., Gomez-Sanchez, C., and Rafestin-Oblin, M. (1999) Specific hydroxylations determine selective corticosteroid recognition by human glucocorticoid and mineralocorticoid receptors. *FEBS Lett.* **464**, 9–13
8. Fagart, J., Wurtz, J. M., Souque, A., Hellal-Levy, C., Moras, D., and Rafestin-Oblin, M. E. (1998) Antagonism in the human mineralocorticoid receptor. *EMBO J.* **17**, 3317–3325
9. Funder, J. (2017) 30 years of the mineralcorticoid receptor: mineralocorticoid receptor activation and specificity-conferring mechanisms: a brief history. *J. Endocrinol.* **234**, T17–T21

10. Funder, J. W., Pearce, P. T., Smith, R., and Smith, A. I. (1988) Mineralocorticoid action: target tissue specificity is enzyme, not receptor, mediated. *Science* **242**, 583–585
11. Odermatt, A., and Atanasov, A. G. (2009) Mineralocorticoid receptors: emerging complexity and functional diversity. *Steroids* **74**, 163–171
12. Funder, J., and Myles, K. (1996) Exclusion of corticosterone from epithelial mineralocorticoid receptors is insufficient for selectivity of aldosterone action: *in vivo* binding studies. *Endocrinology* **137**, 5264–5268
13. Funder, J. W. (2007) Mineralocorticoid receptor activation and oxidative stress. *Hypertension* **50**, 840–841
14. Oakley, R. H., and Cidlowski, J. A. (2013) The biology of the glucocorticoid receptor: new signaling mechanisms in health and disease. *J. Allergy Clin. Immunol.* **132**, 1033–1044
15. Fuller, P. J., Lim-Tio, S. S., and Brennan, F. E. (2000) Specificity in mineralocorticoid versus glucocorticoid action. *Kidney Int.* **57**, 1256–1264
16. Pascual-Le Tallec, L., Simone, F., Viengchareun, S., Meduri, G., Thirman, M. J., and Lombès, M. (2005) The elongation factor ELL (eleven-nineteen lysine-rich leukemia) is a selective coregulator for steroid receptor functions. *Mol. Endocrinol.* **19**, 1158–1169
17. Berger, S., Bleich, M., Schmid, W., Cole, T. J., Peters, J., Watanabe, H., Kriz, W., Warth, R., Greger, R., and Schütz, G. (1998) Mineralocorticoid receptor knockout mice: pathophysiology of Na^+ metabolism. *Proc. Natl. Acad. Sci. USA* **95**, 9424–9429
18. Cole, T. J., Blendy, J. A., Monaghan, A. P., Krieglstein, K., Schmid, W., Aguzzi, A., Fantuzzi, G., Hummler, E., Unsicker, K., and Schütz, G. (1995) Targeted disruption of the glucocorticoid receptor gene blocks adrenergic chromaffin cell development and severely retards lung maturation. *Genes Dev.* **9**, 1608–1621
19. Gumz, M. L., Stow, L. R., Lynch, I. J., Greenlee, M. M., Rudin, A., Cain, B. D., Weaver, D. R., and Wingo, C. S. (2009) The circadian clock protein Period 1 regulates expression of the renal epithelial sodium channel in mice. *J. Clin. Invest.* **119**, 2423–2434
20. Reddy, T. E., Pauli, F., Sprouse, R. O., Neff, N. F., Newberry, K. M., Garabedian, M. J., and Myers, R. M. (2009) Genomic determination of the glucocorticoid response reveals unexpected mechanisms of gene regulation. *Genome Res.* **19**, 2163–2171
21. Le Billan, F., Khan, J. A., Lamribet, K., Viengchareun, S., Bouligand, J., Fagart, J., and Lombès, M. (2015) Cistrome of the aldosterone-activated mineralocorticoid receptor in human renal cells. *FASEB J.* **29**, 3977–3989
22. Prié, D., Friedlander, G., Coureau, C., Vandewalle, A., Cassingéna, R., and Ronco, P. M. (1995) Role of adenosine on glucagon-induced cAMP in a human cortical collecting duct cell line. *Kidney Int.* **47**, 1310–1318
23. Deppe, C. E., Heering, P. J., Viengchareun, S., Grabensee, B., Farman, N., and Lombès, M. (2002) Cyclosporine a and FK506 inhibit transcriptional activity of the human mineralocorticoid receptor: a cell-based model to investigate partial aldosterone resistance in kidney transplantation. *Endocrinology* **143**, 1932–1941
24. Amazit, L., Le Billan, F., Kolkhof, P., Lamribet, K., Viengchareun, S., Fay, M. R., Khan, J. A., Hillisch, A., Lombès, M., Rafestin-Oblin, M.-E., and Fagart, J. (2015) Finerenone impedes aldosterone-dependent nuclear import of the mineralocorticoid receptor and prevents genomic recruitment of steroid receptor coactivator-1. *J. Biol. Chem.* **290**, 21876–21889
25. Fagart, J., Huyet, J., Pinon, G. M., Rochel, M., Mayer, C., and Rafestin-Oblin, M.-E. (2005) Crystal structure of a mutant mineralocorticoid receptor responsible for hypertension. *Nat. Struct. Mol. Biol.* **12**, 554–555
26. Fagart, J., Seguin, C., Pinon, G. M., and Rafestin-Oblin, M.-E. (2005) The Met852 residue is a key organizer of the ligand-binding cavity of the human mineralocorticoid receptor. *Mol. Pharmacol.* **67**, 1714–1722
27. Travers, S., Martinerie, L., Bouvattier, C., Boileau, P., Lombès, M., and Pussard, E. (2017) Multiplexed steroid profiling of gluco- and mineralocorticoids pathways using a liquid chromatography tandem mass spectrometry method. *J. Steroid Biochem. Mol. Biol.* **165**, 202–211
28. Bärfacker, L., Kuhl, A., Hillisch, A., Grosser, R., Figueroa-Pérez, S., Heckroth, H., Nitsche, A., Ergüden, J.-K., Gielen-Haertwig, H., Schlemmer, K.-H., Mittendorf, J., Paulsen, H., Platzek, J., and Kolkhof, P. (2012) Discovery of BAY 94-8862: a nonsteroidal antagonist of the mineralocorticoid receptor for the treatment of cardiorenal diseases. *ChemMedChem* **7**, 1385–1403
29. Schreiber, J. R., Hsueh, A. J., and Baulieu, E. E. (1983) Binding of the anti-progestin RU-486 to rat ovary steroid receptors. *Contraception* **28**, 77–85
30. Petit-Topin, I., Fay, M., Resche-Rigon, M., Ulmann, A., Gainer, E., Rafestin-Oblin, M. E., and Fagart, J. (2014) Molecular determinants of the recognition of ulipristal acetate by oxo-steroid receptors. *J. Steroid Biochem. Mol. Biol.* **144**, 427–435
31. Viengchareun, S., Kamenicky, P., Teixeira, M., Butlen, D., Meduri, G., Blanchard-Gutton, N., Kurschat, C., Lanel, A., Martinerie, L., Sztal-Mazer, S., Blot-Chabaud, M., Ferrary, E., Cherradi, N., and Lombès, M. (2009) Osmotic stress regulates mineralocorticoid receptor expression in a novel aldosterone-sensitive cortical collecting duct cell line. *Mol. Endocrinol.* **23**, 1948–1962
32. Viengchareun, S., Lema, I., Lamribet, K., Keo, V., Blanchard, A., Cherradi, N., and Lombès, M. (2014) Hypertonicity compromises renal mineralocorticoid receptor signaling through Tis11b-mediated post-transcriptional control. *J. Am. Soc. Nephrol.* **25**, 2213–2221
33. Richards, J., Jeffers, L. A., All, S. C., Cheng, K.-Y., and Gumz, M. L. (2013) Role of Per1 and the mineralocorticoid receptor in the coordinate regulation of αENaC in renal cortical collecting duct cells. *Front. Physiol.* **4**, 253
34. Richards, J., Ko, B., All, S., Cheng, K.-Y., Hoover, R. S., and Gumz, M. L. (2014) A role for the circadian clock protein Per1 in the regulation of the NaCl co-transporter (NCC) and the with-no-lysine kinase (WNK) cascade in mouse distal convoluted tubule cells. *J. Biol. Chem.* **289**, 11791–11806
35. Conway-Campbell, B. L., Pooley, J. R., Hager, G. L., and Lightman, S. L. (2012) Molecular dynamics of ultradian glucocorticoid receptor action. *Mol. Cell. Endocrinol.* **348**, 383–393
36. Fujihara, Y., Kondo, H., Noguchi, T., and Togari, A. (2014) Glucocorticoids mediate circadian timing in peripheral osteoclasts resulting in the circadian expression rhythm of osteoclast-related genes. *Bone* **61**, 1–9
37. Cheon, S., Park, N., Cho, S., and Kim, K. (2013) Glucocorticoid-mediated Period2 induction delays the phase of circadian rhythm. *Nucleic Acids Res.* **41**, 6161–6174
38. Zhang, S., Jonklaas, J., and Danielsen, M. (2007) The glucocorticoid agonist activities of mifepristone (RU486) and progesterone are dependent on glucocorticoid receptor levels but not on EC_{50} values. *Steroids* **72**, 600–608
39. Lombès, M., Binart, N., Delahaye, F., Baulieu, E. E., and Rafestin-Oblin, M. E. (1994) Differential intracellular localization of human mineralocorticosteroid receptor on binding of agonists and antagonists. *Biochem. J.* **302**, 191–197
40. Métivier, R., Penot, G., Hübner, M. R., Reid, G., Brand, H., Kos, M., and Gannon, F. (2003) Estrogen receptor-alpha directs ordered, cyclical, and combinatorial recruitment of cofactors on a natural target promoter. *Cell* **115**, 751–763
41. Métivier, R., Reid, G., and Gannon, F. (2006) Transcription in four dimensions: nuclear receptor-directed initiation of gene expression. *EMBO Rep.* **7**, 161–167
42. Reid, G., Hübner, M. R., Métivier, R., Brand, H., Denger, S., Manu, D., Beaudouin, J., Ellenberg, J., and Gannon, F. (2003) Cyclic, proteasome-mediated turnover of unliganded and liganded ERalpha on responsive promoters is an integral feature of estrogen signaling. *Mol. Cell* **11**, 695–707
43. Takahashi, J. S. (2017) Transcriptional architecture of the mammalian circadian clock. *Nat. Rev. Genet.* **18**, 164–179
44. Weikum, E. R., Knuesel, M. T., Ortlund, E. A., and Yamamoto, K. R. (2017) Glucocorticoid receptor control of transcription: precision and plasticity *via* allostery. *Nat. Rev. Mol. Cell Biol.* **18**, 159–174
45. Stortz, M., Presman, D. M., Bruno, L., Annibale, P., Dansey, M. V., Burton, G., Gratton, E., Pecci, A., and Levi, V. (2017) Mapping the dynamics of the glucocorticoid receptor within the nuclear landscape. *Sci. Rep.* **7**, 6219
46. Phatnani, H. P., and Greenleaf, A. L. (2006) Phosphorylation and functions of the RNA polymerase II CTD. *Genes Dev.* **20**, 2922–2936
47. Chapman, R. D., Heidemann, M., Albert, T. K., Mailhammer, R., Flatley, A., Meisterernst, M., Kremmer, E., and Eick, D. (2007) Transcribing RNA polymerase II is phosphorylated at CTD residue serine-7. *Science* **318**, 1780–1782
48. Welboren, W.-J., van Driel, M. A., Janssen-Megens, E. M., van Heeringen, S. J., Sweep, F. C., Span, P. N., and Stunnenberg, H. G. (2009) ChIP-seq of ERalpha and RNA polymerase II defines genes differentially responding to ligands. *EMBO J.* **28**, 1418–1428

49. Guiochon-Mantel, A., Loosfelt, H., Lescop, P., Sar, S., Atger, M., Perrot-Applanat, M., and Milgrom, E. (1989) Mechanisms of nuclear localization of the progesterone receptor: evidence for interaction between monomers. *Cell* **57**, 1147–1154
50. Savory, J. G., Préfontaine, G. G., Lamprecht, C., Liao, M., Walther, R. F., Lefebvre, Y. A., and Haché, R. J. (2001) Glucocorticoid receptor homodimers and glucocorticoid-mineralocorticoid receptor heterodimers form in the cytoplasm through alternative dimerization interfaces. *Mol. Cell. Biol.* **21**, 781–793
51. Grossmann, C., Ruhs, S., Langenbruch, L., Mildenberger, S., Strätz, N., Schumann, K., and Gekle, M. (2012) Nuclear shuttling precedes dimerization in mineralocorticoid receptor signaling. *Chem. Biol.* **19**, 742–751
52. Ou, X. M., Storring, J. M., Kushwaha, N., and Albert, P. R. (2001) Heterodimerization of mineralocorticoid and glucocorticoid receptors at a novel negative response element of the 5-HT1A receptor gene. *J. Biol. Chem.* **276**, 14299–14307
53. Mifsud, K. R., and Reul, J. M. H. M. (2016) Acute stress enhances heterodimerization and binding of corticosteroid receptors at glucocorticoid target genes in the hippocampus. *Proc. Natl. Acad. Sci. USA* **113**, 11336–11341
54. Watson, L. C., Kuchenbecker, K. M., Schiller, B. J., Gross, J. D., Pufall, M. A., and Yamamoto, K. R. (2013) The glucocorticoid receptor dimer interface allosterically transmits sequence-specific DNA signals. *Nat. Struct. Mol. Biol.* **20**, 876–883
55. Pippal, J. B., Yao, Y., Rogerson, F. M., and Fuller, P. J. (2009) Structural and functional characterization of the interdomain interaction in the mineralocorticoid receptor. *Mol. Endocrinol.* **23**, 1360–1370
56. Presman, D. M., Ganguly, S., Schiltz, R. L., Johnson, T. A., Karpova, T. S., and Hager, G. L. (2016) DNA-binding triggers the tetramerization of the glucocorticoid receptor in live cells. *Proc. Natl. Acad. Sci. USA* **113**, 8236–8241
57. Denker, A., and de Laat, W. (2015) A long-distance chromatin affair. *Cell* **162**, 942–943
58. Tang, Z., Luo, O. J., Li, X., Zheng, M., Zhu, J. J., Szalaj, P., Trzaskoma, P., Magalska, A., Wlodarczyk, J., Ruszczycki, B., Michalski, P., Piecuch, E., Wang, P., Wang, D., Tian, S. Z., Penrad-Mobayed, M., Sachs, L. M., Ruan, X., Wei, C.-L., Liu, E. T., Wilczynski, G. M., Plewczynski, D., Li, G., and Ruan, Y. (2015) CTCF-mediated human 3D genome architecture reveals chromatin topology for transcription. *Cell* **163**, 1611–1627
59. Rowley, M. J., and Corces, V. G. (2016) The three-dimensional genome: principles and roles of long-distance interactions. *Curr. Opin. Cell Biol.* **40**, 8–14
60. Morris, D. J., Latif, S. A., and Brem, A. S. (2009) Interactions of mineralocorticoids and glucocorticoids in epithelial target tissues revisited. *Steroids* **74**, 1–6